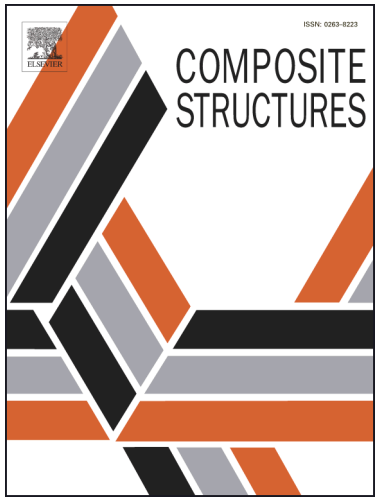

A simplified and fast computational finite element model for the nonlinear load-displacement behaviour of reinforced concrete structures

S. Benakli, Y. Bouafia, M. Oudjene, R. Boissière, A. Khelil

PII: S0263-8223(18)30517-8
DOI: https://doi.org/10.1016/j.compstruct.2018.03.070
Reference: COST 9517

To appear in: *Composite Structures*

Received Date: 14 February 2018
Revised Date: 17 March 2018
Accepted Date: 20 March 2018

Please cite this article as: Benakli, S., Bouafia, Y., Oudjene, M., Boissière, R., Khelil, A., A simplified and fast computational finite element model for the nonlinear load-displacement behaviour of reinforced concrete structures, *Composite Structures* (2018), doi: https://doi.org/10.1016/j.compstruct.2018.03.070

A simplified and fast computational finite element model for the nonlinear load-displacement behaviour of reinforced concrete structures

S. Benakli[1], Y. Bouafia[1], M. Oudjene[2], R. Boissière[3], A. Khelil[3]

[1] Université de Tizi-Ouzou, Laboratoire de Modélisation des Matériaux et Structures de génie civil (LaMoMS), Département de génie-civil, BP 17, 15000 Tizi-Ouzou, Algérie
2 Université de Lorraine, Laboratoire d'Etudes et de Recherche sur le Matériau Bois (LERMAB), 27 rue Philippe Séguin 88026 Epinal, France
3 Université de Lorraine, Institut Jean Lamour (IJL), 2 allée André Guinier, 54011 Nancy, France

Abstract: Numerical simulation of reinforced concrete structures requires the explicit representation of both the concrete and the reinforcement bars, where the two materials are modelled separately using appropriate constitutive laws including damage variables for concrete in compression and tension. Even if this way of modelling is convenient and satisfactory, it requires a huge computational effort especially in the case of large scale applications. The aim of this paper is to develop an alternative model dedicated for the simulation of large scale reinforced concrete structures with no need to represent explicitly the steel reinforcements. Based on the literature review, the authors developed a fictitious stress-strain relationship for reinforced concrete under tension. The model is based on the shape of the slip-adhesion curve between steel and concrete proposed by the European Committee for Concrete (C.E.B.) to estimate the crack opening widths. Relationships covering the cracked stage up to the yield point of the steel are proposed depending on the material properties of concrete and steel, on the reinforcement ratio, as well as on the crack widths. The developed model was successfully implemented in the ABAQUS commercial software. The effectiveness and computational efficiency are demonstrated through some examples under tensile and bending loadings.

Keywords: concrete, steel reinforcement, crack opening, bond-slip, FEM

1. Introduction

The design process of reinforced concrete (RC) structures is generally governed by the ultimate compressive crushing strength of concrete, while the tensile loading is assumed to be carried by steel reinforcements. Thus, cracking of concrete under tensile loading is expected to occur already in the service state and cannot be avoided in most structural engineering applications. On the other hand, taking into account the contribution of the tensile zone of the concrete, in the cracked stage, to the global stiffness of the entire reinforced concrete element is one way to describe more closely the real behavior of reinforced concrete structures and so to increase the robustness and capabilities of the computational methods.

Cracking of concrete under tensile loading is a complex phenomenon which leads to progressive reduction of the stiffness of the reinforced concrete structural element. The stiffness reduction is generally a combination between cracking of concrete under tension and the local loss of the bond (adhesion) between steel bar and concrete at a fully cracked section. It is, therefore, of primary importance to accurately model and predict the stiffness reduction during the cracked stage for a proper design of structural engineering applications.

Extensive experimental and numerical studies on both small-scale and full-scale RC beams and walls have been published in the literature. In these studies the finite element method is the widely used approach to predict the behaviour of the RC elements based on 3D continuum mechanics [1-8], among others. Usually, there are two main strategies: (1) both the concrete element and the steel

reinforcement are modelled separately using 3D solid finite elements using different constitutive laws (for concrete and steel), where the imperfectly bond-slip relationship between steel reinforcement and concrete is accounted for, (2) the concrete element is modelled using 3D solid finite elements while the steel reinforcement is modelled using 1D bar elements, where the interaction between concrete and steel reinforcement is modelled as embedded condition. Even if the first strategy is more complex and cost expensive, its main advantage by comparison to the former one is the prediction of the relative slip between concrete and steel reinforcement. In both strategies, the well-known concrete damage plasticity model (CDPM), available in Abaqus software [9], is widely used to predict the bahaviour of concrete under compression and tension, including damage variables for both compression and tension, while the steel reinforcements are assumed as isotropic elasto-plastic material model.

These strategies are generally satisfactory and convenient when dealing with relatively smaller individual structural elements (beams, columns). However, in the case of large-scale concrete structures (multi-story portal frames, shear walls, etc.) the computational effort would be huge due to the explicit detailed modelling of the steel reinforcements as well as the local degradation phenomena (progressive cracking of concrete, relative slip between concrete and steel). It can be concluded, therefore, that the computational effort is a key point for engineers and modellers in the choice of the modelling approach to adopt.

The building codes (C.E.B., Eurocode 2, etc.) suggest to evaluation and to limit the crack opening in the service state using simplified formulas, depending on both the mean steel and concrete strains between two successive cracks [10-11], to avoid corrosion of the steel reinforcements. On the other hand, several experimental and analytical studies dealing with the stiffness of RC elements under tension are available in the literature [12,17-21]. A comprehensive review of the relevant existing analytical models proposed in the literature to assess the load-mean strain curve of a RC element under tension in the cracked stage is given in [12]. These models are mostly based on the relationship between the mean RC strain and the steel strain in a fully cracked section.

The main purpose of this paper is to develop a fast and simplified predictive model to simulate the global behaviour of RC structures dedicated to large scale applications with no need to represent explicitly the reinforcement bars in the model neither the progressive damage of concrete in tension. To this end, a fictitious tension behaviour model for the RC, where the physics involved in the reinforced concrete, namely relative slip between concrete and reinforcement, at a fully cracked section, as well as the crack opening widths, are explicitly accounted for in the developed fictitious constitutive stress-strain relationship. The requirements due to both the simplicity and the predictivity (accuracy) of the finite element model are considered of primary importance. The developed model was successfully implemented in the Abaqus finite element code to simulate some examples including both tensile and bending loadings.

2. Finite element modelling

2.1. Stiffness of RC in the cracked stage

When a RC element is subjected to tension, two main stages can be distinguished: (1) linear elastic stage (without cracks) and (2) inelastic cracked stage (Fig. 1). In the first stage, the overall behavior is almost linear elastic, until the concrete reaches its tensile strength limit (point A, Fig.1). This stage exhibits a much higher stiffness by comparison to the stiffness of the individual steel bar (line OB, Fig.1), thanks to the contribution of the tensile stiffness of the concrete to the global stiffness of the entire RC element. In the second stage (beyond the point A), as loading of the RC element increases

cracks take place progressively in the concrete section and the tensile applied loading is redistributed along the entire RC element thanks to the bond-slip shear stress between concrete and steel. The cracked stage is characterized by the number of the developed cracks and their opening widths. This stage is accompanied with a gradually decrease of the global stiffness of the loaded RC element, until it reaches the stiffness of the individual steel bars.

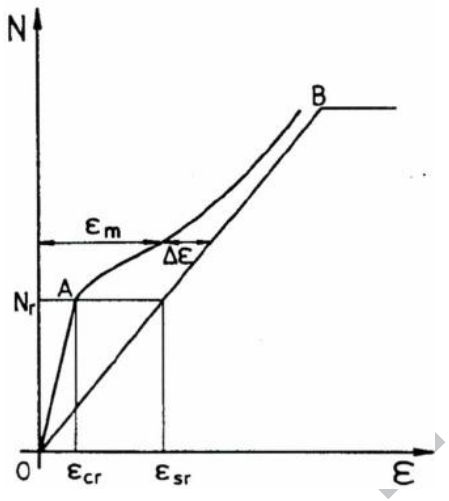

Fig. 1: Load-mean strain curve of RC under tension [12].

The literature review shows that one common point of the existing models dealing with the stiffness of RC during the cracked stage is that they are based on the relation between the mean strain of the RC (ε_m) and the steel strain (ε_s) in a fully cracked cross-section, which can be expressed as follows [12]:

$$_m = \ _s - \Delta\varepsilon \quad (1)$$

where$\Delta\varepsilon$ stands for the tension stiffening effect of concrete lying between two successive cracks.

2.2. Fictitious behaviour of RC under tension

The proposal of the present paper is to establish the relationship between the applied tension load and the mean strain ε_{cm} of the RC element subjected to tension. The constitutive law (stress-strain curve) can be obtained by dividing the total tensile load by the equivalent and homogenized concrete cross-section. Here, the developed model for RC in tension is briefly discussed. The readers can refer to [22, 23, 27] for a better reading on the theoretical aspects.

In the present study, the behaviour of a RC under tension is assumed to follow three main stages (Fig. 2), namely linear elastic stage (branch OA), inelastic cracked stage (branch AC) and elastic cracked stage (CB).

The different relations and computing methods covering the three stages described above are given hereafter.

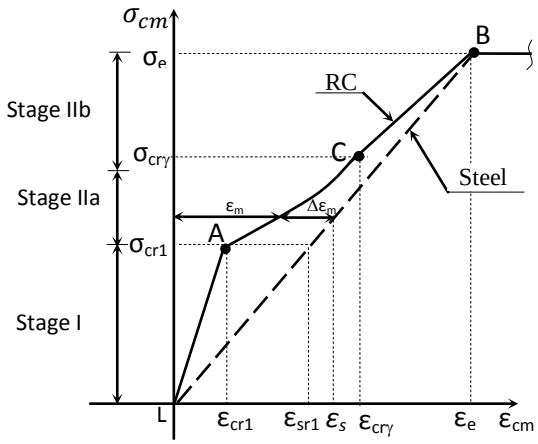

Fig. 2: Stress-strain relationship of reinforced concrete under tension

2.2.1. Bond-slip relationship ($\tau - g$)

The goal of this section is to estimate the mean strain of the RC element induced by the relative slip between the steel bars and concrete at a fully cracked cross-section.

Let's consider the introduction length l_t and disturbed length l_0 [13-16] (Fig. 4), such that $l_0 = \delta l_t$ ($\delta = 0.10 \sim 0.20$) [13]. Thus, the effective introduction length is $(l_t - l_0) = (1 - \delta) l_t$.

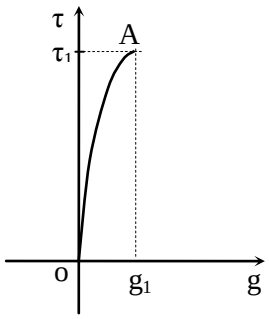

Fig. 3: The τ-g curve proposed by the C.E.B.

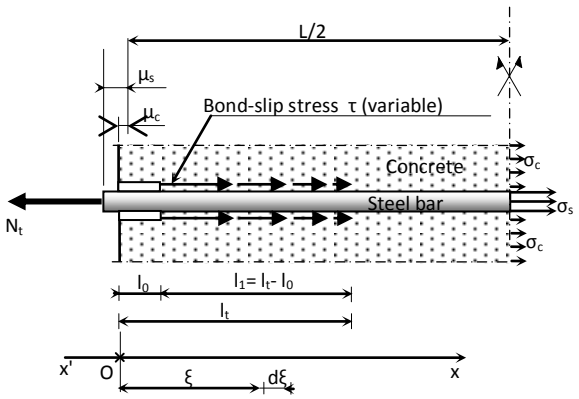

Fig. 4: Relative slip g (= μs-μc) and distribution of the bond-slip shear stress

The equilibrium equation of a steel bar embedded in a concrete block (Fig. 4) can be written as follows:

$$\sigma_s(X) = \sigma_{sf} - \int_0^X \frac{p}{A_s}\tau(\xi)d\xi \tag{2}$$

The corresponding steel strain can be expressed as follows:

$$_s(X) = \ _{sf} - \int_0^X \frac{p}{E_s A_s}\tau(\xi)d\xi \tag{3}$$

$$\frac{d\varepsilon_s}{dX} = -\frac{p}{E_s A_s}\tau(X) \tag{4}$$

The relative slip between steel and concrete can be expressed as follows:

$$g(X) = u_c(X) - u_s(X) \tag{5}$$

The first and second derivatives of the relation (5) lead to:

$$\frac{dg}{dX} = \frac{du_c}{dX} - \frac{du_s}{dX} = \ _c - \ _s \tag{6}$$

$$\frac{d^2g}{dX^2} = \frac{d\varepsilon_c}{dX} - \frac{d\varepsilon_s}{dX} \tag{7}$$

For a given concrete cross-section between two successive cracks, the concrete stress and strain can be expressed respectively as:

$$\sigma_c(X) = \frac{p}{(A_c - A_s)} \int_0^X \tau(\xi) d\xi \tag{8}$$

$$_c(X) = \frac{p}{E_s A_s} \frac{n\rho}{(1-\rho)} \int_0^X \tau(\xi) d\xi \tag{9}$$

From the equation (9), it can be written:

$$\frac{d\varepsilon_c}{dX} = \frac{p}{E_s A_s} \frac{n\rho}{(1-\rho)} \tau(X) \tag{10}$$

By substituting equations (3-4) and (9-10) in the equation (7), we obtain the differential equation (11) governing the relative slip g, between steel and concrete:

$$\frac{d^2g}{dx^2} - \frac{p}{A_s E_s \overline{\rho}} \tau(x) = 0 \tag{11}$$

The expression (11) is used to establish, in the domain $[l_0,\ l_t]$, the different quantities $_c(x),\ g(x), \tau(x)$ and $_s(x)$ as a function of x along the effective introduction length l_t.

In the present study, we limit ourselves to a value of relative slip $g \leq g_1$(Fig. 3). If we consider the effective introduction length $l_1 = l_t - l_0$, the solution of the differential equation (11) is given by [1,5]:

$$g(x) = \theta^{1/(1-\alpha)} [l_1 - x]^{2/(1-\alpha)} \tag{12}$$

where: $\theta = \frac{\beta_1^2 (1-\alpha)^2}{2(1+\alpha)}$; $\beta_1 = \sqrt{\frac{k_1 p}{E_s A_s \overline{\rho}}}$; $k_1 = \frac{\tau_1}{g_1^{\alpha}}$

Using the variable $X = x - l_0$, the variation of the bond slip shear stress along $l_1$can be written as:

$$\tau(X) = k_1 \theta^{\alpha/(1-\alpha)} [l_1 - X]^{2\alpha/(1-\alpha)} \tag{13}$$

By substituting the expression of $\tau(x)$ in the equation (2) and by means the mean value along l_t, we obtainthe mean strain in both the steel bar (ε_{smt1}) and in the concrete (ε_{cmt1}) at the first crack as follows [22]:

$$\varepsilon_{smt1} = \left[\delta + (1+\delta)\left(1 - \frac{1+\alpha}{2}\right)\overline{\rho}\right] \varepsilon_{sf}, \quad \delta = \frac{l_0}{l_t} = 0.1 \tag{14}$$

$$\varepsilon_{cmt1} = (1-\delta)(1-\overline{\rho}) \frac{1+\alpha}{2} \ _{sf} \tag{15}$$

2.2.2. *Linear elastic stage (branch OA)*

Before crack initiation, the behaviour of the RC element is regarded as homogeneous linear elastic material model and the equilibrium equation under tension leads to:

$$N_t = \sigma_c(A_c - A_s) + n\,\sigma_c\,A_s \tag{16}$$

where $n = \frac{E_s}{E_c}$

The mean concrete strain is obtained from the equation (11) as follows:

$$_{cm} = \ _{cr1} = \varepsilon_s = \frac{\sigma_c}{E_c} = \frac{\Delta L}{L} = \frac{N_t(1-\overline{\rho})}{E_s A_s} \tag{17}$$

where $\overline{\rho} = 1/\left(1 + \frac{n\rho}{1-\rho}\right)$ and $\rho = A_s/A_c$

2.2.3. *Inelastic cracked stage (branch AC)*

This stage starts at the onset of the first crack. This is likely to appear in a section corresponding to the weakest point of the concrete in tension, leading to a variation of the tensile strength of the concrete along the entire RC element. Moving away from either side of this first crack, the applied tensile force (N_t) is progressively transmitted to the concrete thanks to the steel-concrete adhesion. Further cracks appear progressively as the tensile loading increases. This stage (branch *AC*) stops when the cracking becomes stable (number of cracks is stable).

The literature dealing with the progressive formation of the concrete cracks [22,23,27] reports the idealized crack propagation shown in Fig. 5. From this figure, it can be observed that as long as the number of cracks remains lower that $\gamma/2$ (Fig. 5a), the introduction length l_t may change. Beyond, every formation of new crack takes place at equidistance (denoted $\overline{\lambda}$) between two successive cracks (Fig. 5b).

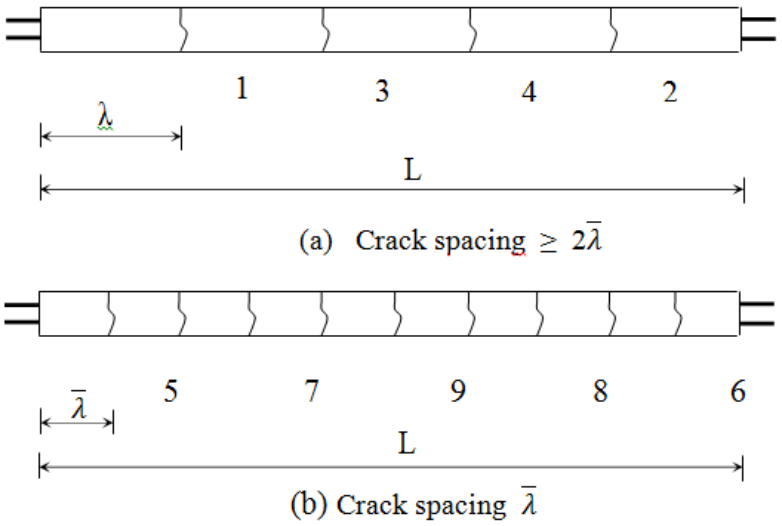

Fig. 5: Idealized progressive formation of cracks

In this stage, one distinguishes two cases:

a) Case 1: $\lambda > 2\, l_t$

Here, it is assumed that the relative slip between steel and concrete is lower than the value g_1 corresponding to the maximum bond-shear stress τ_1 (Fig. 3), such that:

$$\tau = \tau_1 \left(\frac{g}{g_1}\right)^{\alpha} \tag{18}$$

The parameter α is ranged from 0.25 to 0.40 according the concrete confinement [10].

The parameter λ denotes the spacing between two successive cracks before the stabilization state of the crack propagation, such that $\lambda > 2l_t$ (where $l_t = l_0 + l_1$). At the relative slip g_1, λ is denoted λ_1 and the introduction length $l_t = l_{t1} = l_0 + l_1$.

In the following, $(i = 1)$ and $(i = \gamma)$ denote respectively the first crack and the last crack. During the propagation of cracks, at the crack number i the cracking concrete stress can be expressed as (by assuming $\Delta\eta = \pm 20\%,\ \eta_1 = 0.8,\ \eta_\gamma = 1.2$ [22]):

$$\sigma_{cri} = \eta_i f_{ctm} \tag{19}$$

$$_{cri} = \frac{\eta_i f_{ctm}}{E_c} \tag{20}$$

In this way, the first crack must take place inside the interval $[l_t\ ;\ L - l_t]$. Just before the crack i, with the help of the equation (17) it can be written:

$$_{sri} = \frac{\varepsilon_{cri}}{(1-\overline{\rho})} = \frac{\eta_i f_{ctm}}{E_c(1-\overline{\rho})} = \frac{\eta_i}{\eta_\gamma}\ _{sr\gamma} \tag{21}$$

where $_{sr\gamma} = \frac{\eta_\gamma f_{ctm}}{E_c(1-\overline{\rho})}$

The mean crack spacing λ is taken equal to 1.5 times the effective introduction length at the last main crack ($l_{tr\gamma}$) [24] to allow the formation of all cracks:

$$\lambda = \mu l_{tr\gamma} \tag{22}$$

where $\mu \approx 1.45 - 1.55$

$$l_{tr\gamma} = \frac{1}{(1-\delta)} \left[\frac{(1-\alpha)\varepsilon_{sr\gamma}}{2\theta^{1/(1-\alpha)}}\right]^{(1+\alpha)/(1-\alpha)} \tag{23}$$

Thanks to the mean strain, in the concrete, at a fully cracked section $_{cmt1}$ (see equation (15) and mean strain (ε_{cr1}) of the concrete between two successive cracks calculated using the relation (20), it can be written:

$$\Delta l_{t1} = 2(\varepsilon_{cmt1}.\, l_{tr1}) \tag{24}$$

$$\Delta L_{h1} = \ _{cr1}.\, L_{h1} \tag{25}$$

The effective introduction lengths at the first crack, l_{tr1} and L_{h1} may be calculated, respectively as follows (Fig. 6):

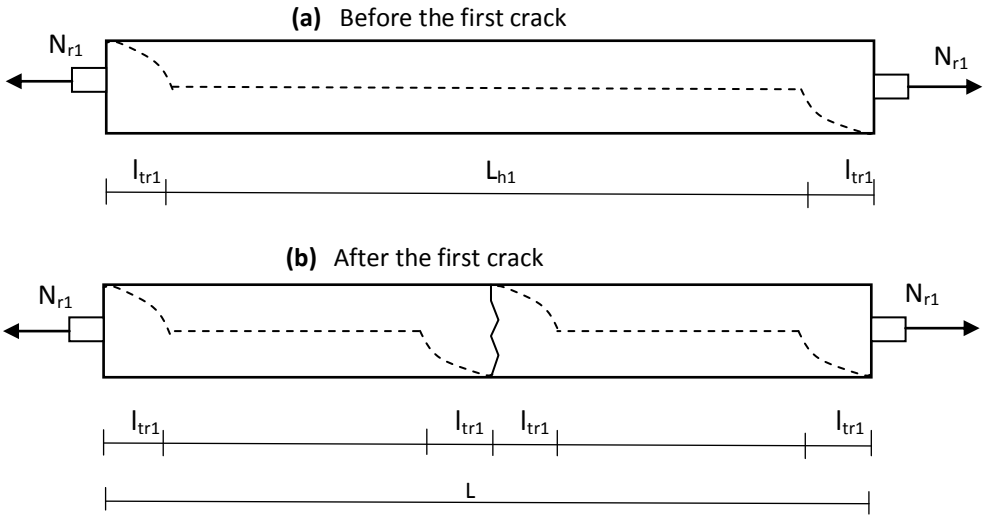

Fig. 6: Formation of the first crack and idealized effective length
(dashed line: distribution of the bond-slip stress)

$$l_{tr1} = \frac{1}{(1-\delta)}\left[\frac{(1-\alpha)\varepsilon_{sr1}}{2\theta^{1/(1-\alpha)}}\right]^{(1+\alpha)/(1-\alpha)} \tag{26}$$

$$L_{h1} = L - 2l_{tr1} \tag{27}$$

The mean strain of the RC element (Fig. 7) for the total introduction length l_t, can be calculated as the sum of the different relative displacements (Δl_{t1}, ΔL_{h1}) divided by its total length (L):

$$cm1 = \frac{\Delta L_1}{L} = \frac{\Delta l_{t1} + \Delta L_{h1}}{L} \tag{28}$$

Finally, the mean strain of the RC element (Fig. 7) for the total introduction length $l_t = l_{t1}$, is obtained using the relation (15).

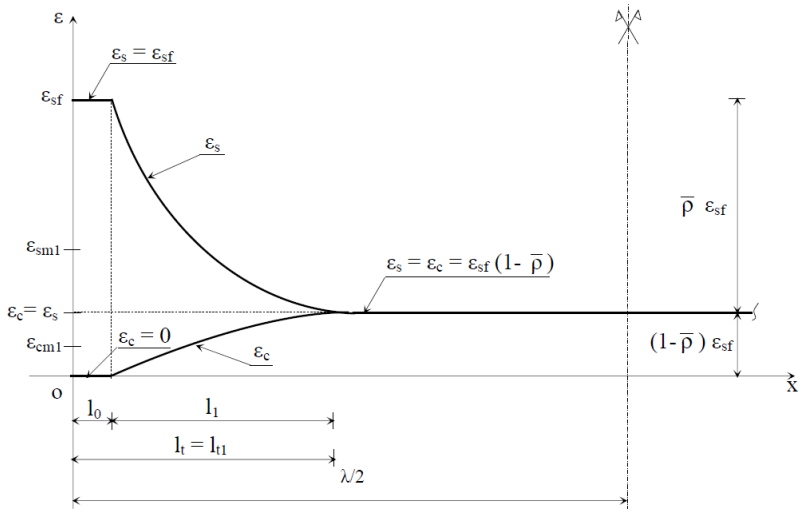

Fig. 7: Distribution of steel and concrete mean strains along the RC element for $g(l_0) < g_1$:
Case when $l_t < \lambda/2$

b) Case 2: $\lambda < 2\, l_{t1}$

Here, γ is used to define the total number of cracks long the entire length of the RC element. This second case starts at the crack number $\gamma/2$ for an even number of cracks and $(\gamma+1)/2$ for an odd number of cracks.

At the stabilization of the crack formation, the effective introduction length l_{1r} decreases. The length l_{1r} is denoted l_{a1}, where the subscript "a" is used to define the stabilization of cracks, such that:

$$\overline{\lambda_1} = 2(l_0 + l_{a1}) = 2\mathrm{l}_{\mathrm{ta1}} \tag{29}$$

$$l_{a1} = \frac{\overline{\lambda_1}}{2}(1-\delta) \tag{30}$$

where $l_0 = \delta\overline{\lambda_1}/2$ and $\overline{\lambda_1} = 1.7\, l_{tr}$

The introduction length l_{tr} and the steel strain $_{sf}$ at a fully cracked section are substituted respectively by l_{ta1} and ε_{sfa1}, such that:

$$\varepsilon_{sfa1} = \left[\frac{2}{(1-\alpha)}\theta^{1/(1-\alpha)} l_{a1}^{(1+\alpha/1-\alpha)}\right] \tag{31}$$

where ε_{sfa1} stands to the mean steel strain at a fully cracked section, in the crack stabilization state, corresponding to the effective introduction length l_{ta1} (Fig. 8).

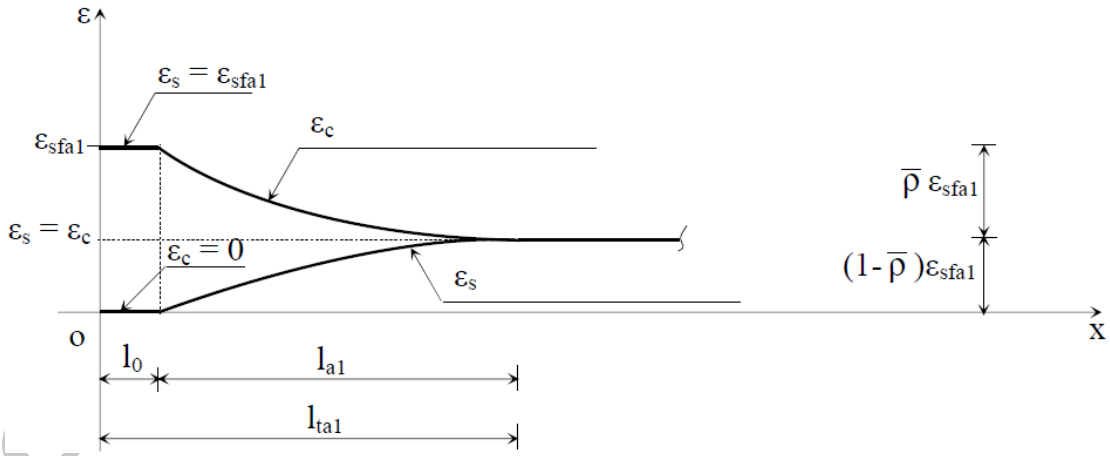

Fig. 8: Distribution of steel and concrete mean strains along the RC element for $g(l_0) < g_1$: Case when $l_t > \lambda/2$

Finally, the mean steel and mean concrete strains, in the stabilized cracked state, are calculated, respectively, as follows:

$$_{smt\overline{\lambda_1}} = \varepsilon_{sf} - \left[(1-\delta)\left(\frac{1+\alpha}{2}\right)\overline{\rho}\,\varepsilon_{sfa1}\right] \tag{32}$$

$$_{cmt\overline{\lambda_1}} = (1-\delta)(1-\overline{\rho})\frac{1+\alpha}{2}\ _{sfa1} \tag{33}$$

It is worth noting that, the second order Lagrange Polynomial is used to compute the shape of the stress-strain curve covering this stage (branch *AC*).

2.2.4. Elastic cracked stage (branch CB)

This stage is characterized by the stability of cracking (the number of cracks likely to form is stable). As the tensile loading N_t increases, the opening width of cracks increases. The stress-strain behaviour in this stage is assumed to increase linearly up to the yield point of the steel bars.

The general flowchart of the computational model is given in Fig. 9.

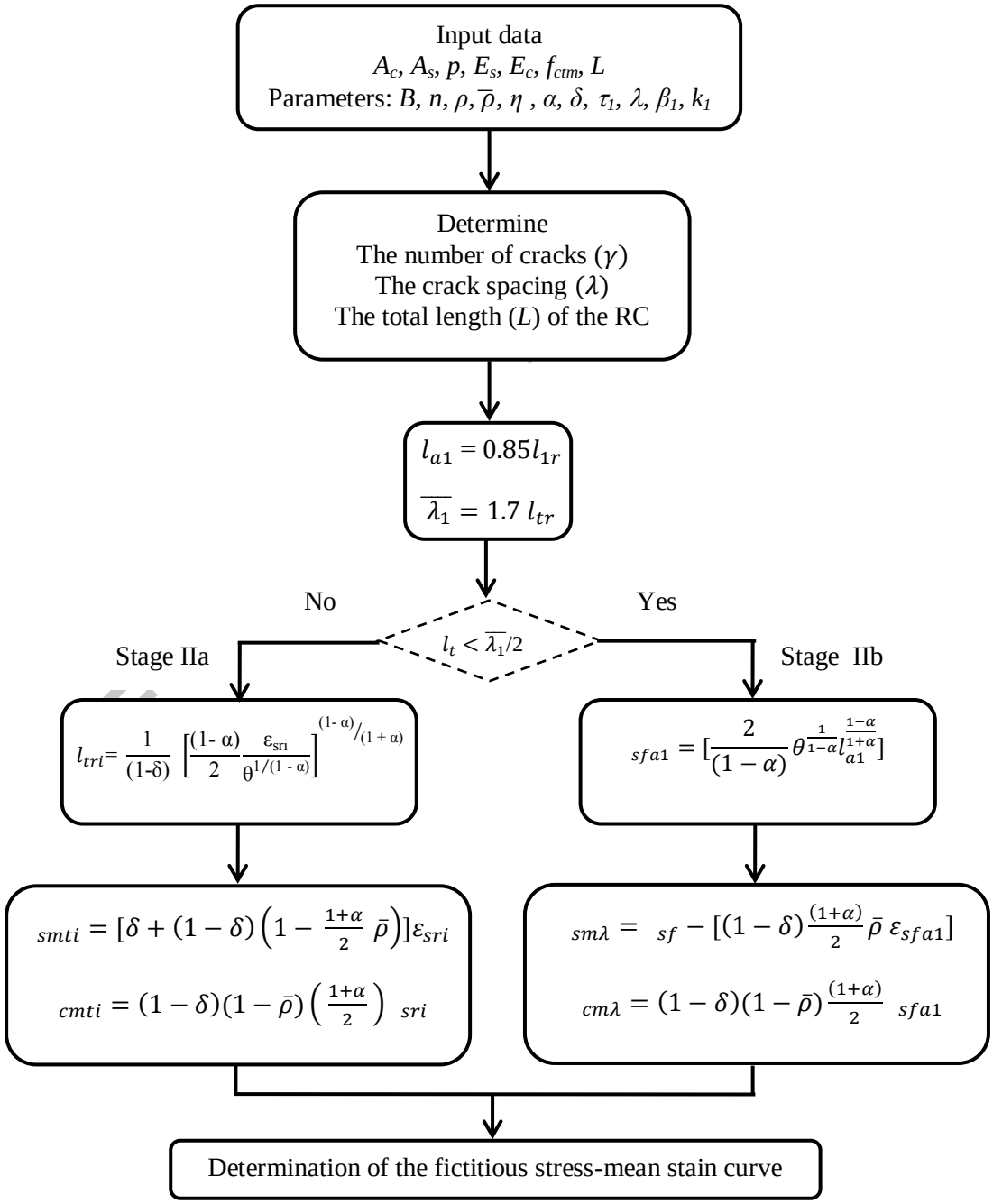

Fig. 9: General flowchart of the calculation model

3. Numerical applications

3.1. Simulation of RC prisms under tension

The first example, described in Fig. 10, is a reinforced concrete prism subjected to tensile loading at the two ends. The RC prism consists of a cross-section of 22500 mm^2 reinforced using 4 steel bars of 12 mm diameter each, leading to a volume fraction steel rebars of 2%. A detailed experimental study of this example, including the development of an analytical model, has been presented earlier by Espion et al. [12].

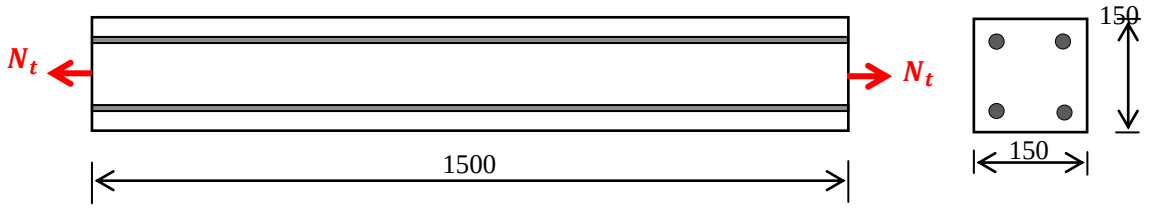

Fig. 10: Geometrical description of the studied RC prism (dimensions in mm)

The global tensile behaviour (load-displacement curve) of the prism is studied numerically and compared to the experimental data from [12].

The prism is modeled using two finite element models (with and without explicit representation of the steel reinforcements):

- Model 1: the concrete is modelled using 3D solid elements based on the concrete damage-plasticity model (CDPM) supported in the Abaqus software, including damage variables in tension. While the steel bars are modelled using truss elements, which are embedded in the concrete, and regarded as isotropic elastoplastic material model (Fig. 11a);
- Model 2: only the concrete is modelled using 3D solid elements (Fig. 11b) and assumed to obey to the developed fictitious stress-strain behaviour under tension (the steel reinforcements are not modelled but their contribution is taken into account implicitly through the fictitious stress-strain curve).

The material properties of the steel reinforcements are: E_s = 200 GPa, ν=0.3 and the yield stress σ_e= 400 MPa. The concrete properties are: E_c = 31.6 GPa, ν=0.13, f_{tm}=1.4 MPa, f_{cm}=34.5 MPa.

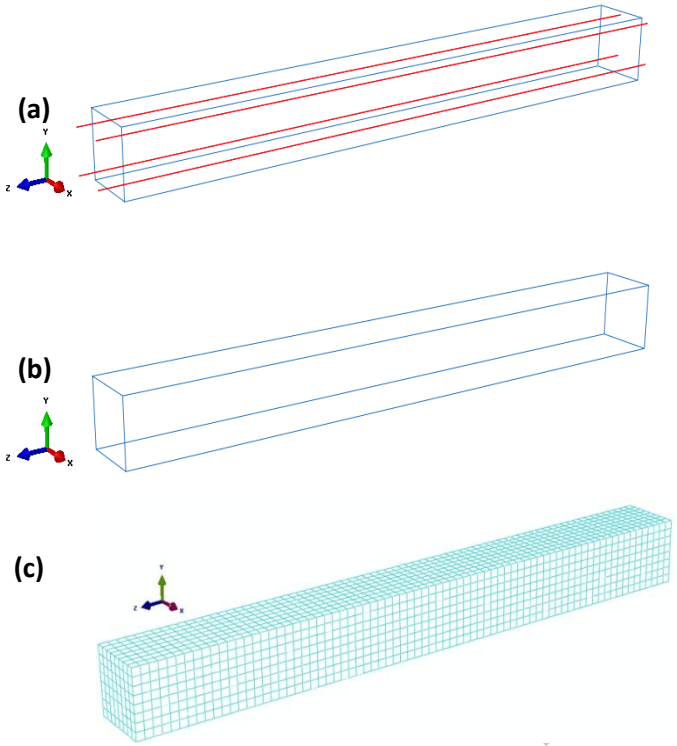

Fig. 11: The different FE models: (a) concrete prism with steel reinforcement (model 1), (b) fictitious concrete prism without steel reinforcement (model 2) and (c) FE mesh of the prism

The numerically-predicted load-displacement curves using both the model 1 and model 2 are compared to the mean experimental curve from [12] (Fig. 12). In addition, the load-displacement curve from the steel bars (4 bars) is plotted for comparison purpose. It can be seen from Fig. 12 that both models 1 and 2 predict well the global behaviour of the RC prism. However, it was observed that the convergence quickness of the model 2 is better as compared to the model 1.

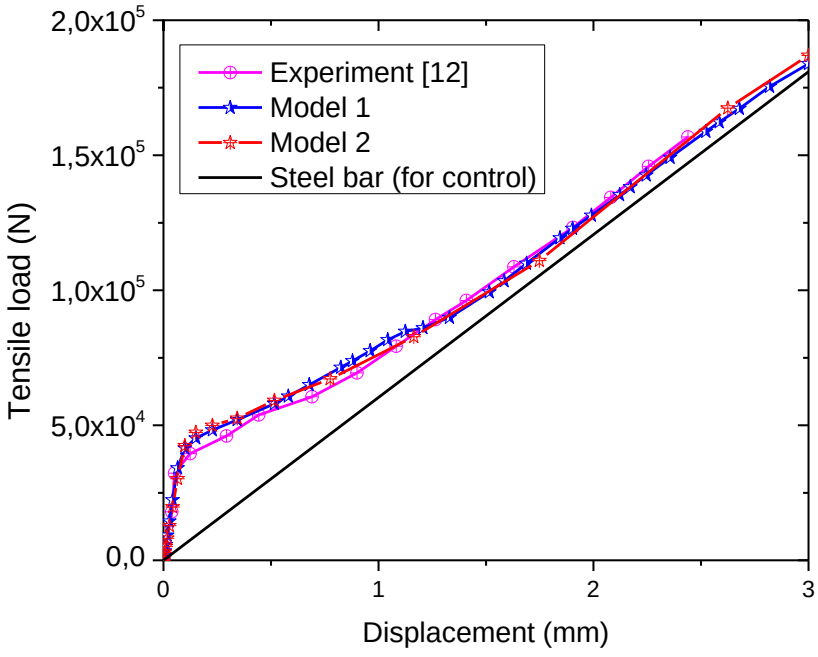

Fig. 12: The numerically-predicted load-displacement curves versus the experimental curve

3.2. Simulation of RC beam under bending

This example involves both experimental and numerical simulation of bending behaviour of a RC beams. The geometrical descriptions of the RC beams as well as the reinfo It is spanne of 15 cm x ormed under ording to the

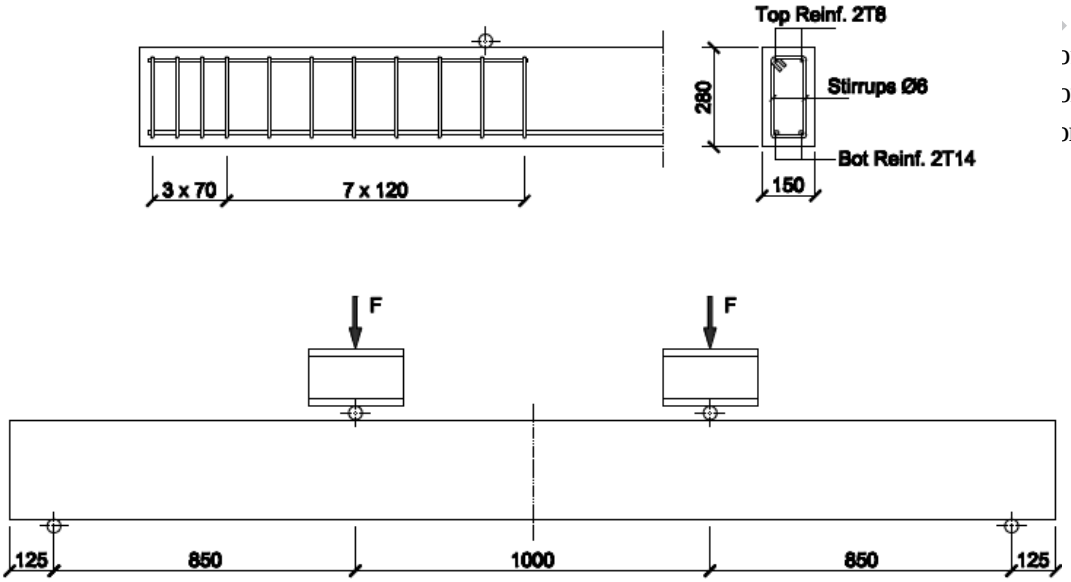

Fig. 13: Geometrical description of the tested RC beams and steel reinforcement layout.

The total applied load was recorded versus the mid-span deflection which is measured using LVDT transducer (Fig. 13).

Fig. 14: Experimental set-up of the RC beam under bending

As in the case of the first example, the numerical simulations were run in two ways:

- Model 1: the RC beam was modelled using 3D continuum mechanics and the streel reinforcements (longitudinal bars and stirrups) were explicitly represented in the model (Fig. 15a);
- Model 2: the RC beam was modelled without the steel reinforcements (Fig. 15b).

In the two models, the concrete was meshed using 3D hexahedral finite elements, as shown in Fig. 15c.

The material properties of the steel reinforcements are: E_s = 210 GPa, ν=0.3 and the yield stress σ_e= 500 MPa. The concrete properties are: E_c = 30 GPa, ν=0.13, f_{tm}=2.1 MPa, f_{cm}= 35 MPa.

The global behaviour of the RC beams was studied and the numerically-predicted load-mid-span deflection curves are compared against the mean experimental curve, showing a fairly good agreement (Fig. 16). It can be seen that both the model 1 and model 2 predict well the global bending behaviour.

It can be observed also from Fig. 16 that the initial global stiffness of the beam (up to about 7 mm deflection) exhibits a slight reduction due to the formation of concrete cracks. The global yielding takes place at about 18 mm deflection and the stiffness of the RC beam held almost constant until complete failure. The main advantages of the model 2 as compared to the model 1 are the quickness and the less pretreatment effort that it requires.

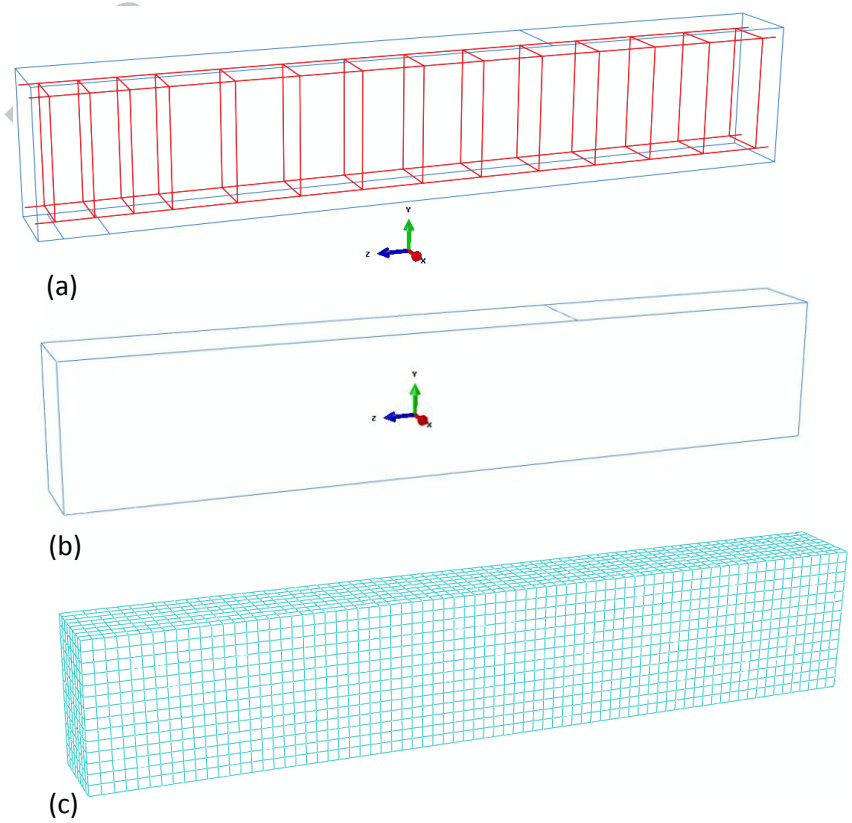

Fig. 15: The different FE models: (a) concrete prism with steel reinforcement (model 1), (b) fictitious concrete prism without steel reinforcement (model 2) and (c) FE mesh of the prism

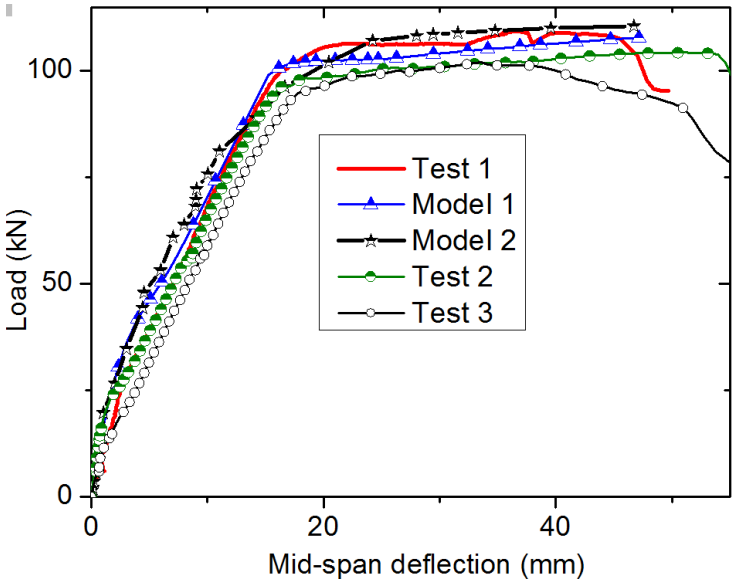

Fig. 16: Numerically-predicted load-deflection curves versus experiments

The tests have been conducted until failure. Cracking of the concrete in the tensile zone the beams (lower face) located between the two loading points (Fig. 17a) was the main observed failure mode. It can be also seen that the model 1 predicts well the formation of the concrete cracks (Fig. 17b). Both experimental observation and numerical simulation show that cracks take place, progressively, as bending load increases, until a certain loading level where compressive damage occurs.

(a) Experimental

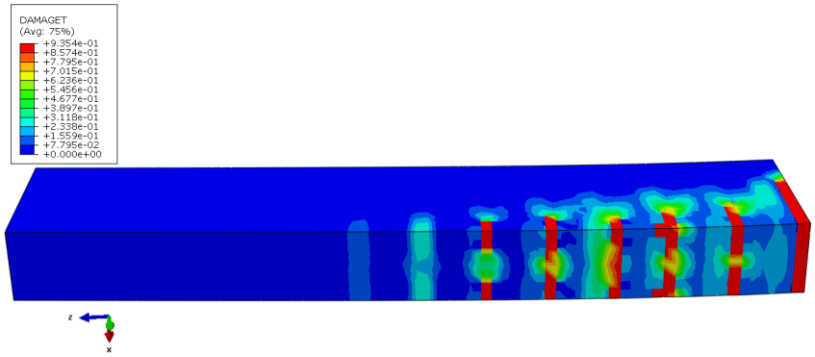

(b) Numerical (one half of the model 1)

Fig. 17: Experimental and numerical concrete crack formation at the lower face of the RC beam

4. Conclusion

Nowadays, the evaluation of the contribution of the concrete stiffness to the reinforced concrete tension element during the cracking stage is becoming increasingly popular. The building codes suggest designing the RC element in such a way to limit the crack opening widths in order to avoid corrosion of steel reinforcements. Several computational models dedicated to the prediction of the tensile stiffness of the RC elements are available in the literature. However, up to now, these models are not explored within the actual context of more and more intensive use of numerical simulation using the finite element method. The aim of this paper was to develop a simplified and fast predictive model to simulate the load-displacement behaviour of RC structures without the need to model the steel reinforcement.

A finite element model that takes into account the degradation of the tensile stiffness of reinforced concrete during the cracking stage has been presented and evaluated for RC prism under tension and RC beam under bending. The model is quite simple and requires much less computational effort because it does not require the explicit representation of the steel reinforcement to evaluate the global behaviour of RC elements.

As an alternative to the existing computational models, the mean stain of the RC is obtained thanks to the relative slip between steel and concrete at a fully cracked section. During the formation of cracks, the redistribution of both the applied tensile load and the bond shear stress along the steel reinforcement bar are evaluated.

The developed model has been successfully implemented in the Abaqus commercial software and successfully applied to study RC element under tensile and bending loadings. The model gives a fairly good agreement as compared to the experimental predictions. The main novelty of the developed model with regard to the existing literature is that there is no need to model the steel reinforcement neither the damage evolution of concrete under tension (as the case in the existing models). Thanks to these characteristics, economical (with regard to the computational effort) simulations are obtained without any divergence problem related to the management of the progressive damage of concrete in tension.

The model, however, needs some complementary verification/developments, namely for its application to full-scale examples. For example, the study of some influential parameters, namely the steel reinforcement ratio, which is an interesting and necessary perspective for the model. Also the

validity domain of the model needs further investigations before obtaining a robust and efficient general computational finite element model.

References

[1] Wei Guo, Wei Fan, Xudong Shao, Dongjie Shen, Baisheng Chen, Constitutive model of ultra-high-performancefiber-reinforced concrete forlow-velocity impact simulations. Composite Structures, Vol. 185, pp. 307-326, 2018.

[2] Wen-rui Yang, Xiong-jun He, Li Dai,Damage behaviour of concrete beams reinforced with GFRP bars. Composite Structures, Vol. 161, pp.173-186, 2017.

[3] Arafa M.A. Ibrahim, Mohamed F.M. Fahmy, Zhishen Wu, 3D finite element modeling of bond-controlled behavior of steel andbasalt FRP-reinforced concrete square bridge columns under lateralloading. Composite Structures,Vol. 143, pp. 33-52, 2016.

[4] C. Mang, L. Jason, L. Davenne, Crack opening estimate in reinforced concrete walls using a steel-concrete bond model. Archives of Civil and Mechanical Engineering, Vol. 16,, pp.422-436, 2016.

[5] C. Mourlas, G. Markou, M. Papadrakakis, 3D nonlinear constitutive modelling for dynamic analysis of reinforced concrete structural members. Procedia Engineering, Vol. 199, pp. 729-734, 2017.

[6] Y. Lu, R. S., Henry, Numerical modelling of reinforced concrete walls with minimum vertical reinforcement. Engineering Structures, Vol. 143, pp. 330-345, 2017.

[7] A. Edalat-Behbahani, J. A. O., Barros, A. Ventura-Gouveia, Three dimensional plastic-damage multidirectional fixed smeared crack approach for modelling concrete structures. Int. J. of Solids and Structures, Vol. 115, pp. 104-125, 2017.

[8] S. Moallemi, S. Pietruszczak, Analysis of localized fracture in 3D reinforced concrete structures using volume averaging technique. Finiteelements in Analysis and Design, Vol. 125, pp.41-52, 2017.

[9] ABAQUS, Theory manual, version 6.2. Hibbit, Karson & Sorensen, Inc.; 2000.

[10] CEB93, Comité Euro -international du Béton/Fédération Internationale de la Précontrainte - CEB-FIP Model Code 1990. Final version published by Thomas Telford Ltd., London, 465 p., 1993.

[11] EN 1992-1-1: Eurocode 2 ‘‘Calcul des Structures en Béton’’ partie 1–1: règlesgénérales et règles pour les bâtiments. Bruxelles; janvier 2004.

[12] B. Espion, M. Provost, P. Halleux, Rigidité d’une zone tendue de béton armé. Matériauxet Construction 0025-5432/85/03 185 07/ 2.70/$, © Bordas-Gauthier-Villars, Vol. 18, pp. 185-191, 1985.

[13] F.F. Ren, Z.F.Yang, J.F.Chen, W. W. Chen, An Analytcal Analysis of the fullrangebehaviour of grouted rockbolts based on a tri-linear bond slip model.Constrution and Building Matérials, Vol. 24, Issue 3, pp. 361-376, March 2010

[14] G. L.Balazs, Cracking analysis based on slip and bond stresses. ACI Materials Journal, July-August 1993, vol. 90, n° 4, p. 340-348.

[15] R. Chaussin, Bases de la théorie de la fissuration, Fissuration et durabilité du béton. Revue Française de Génie Civil, vol. 2, n° 2/1998, p. 243-254.

[16] E. Giuriani, On the effective axial stiffness of a bar in cracked concrete. Bond inConcrete, Ed. Bartos, Applied Science Publishers, London, p. 107-126, 1982.

[17]A. I. Johnson, Deformations of reinforced concrete. Mém.Ass.Int. Ponts Chap., Zurich, vol. 11, pp. 253-290, 1951.

[18] L. Palotas, BeiträgezurBerechnung der Risssicherheit. Mém.Ass.Int. Ponts Chap., Zurich, vol. 26, pp. 365-397, 1966.

[19] R. Favre, M. Koprna, J. C. Putallaz, Deformation of concrete structures.Theoritical basis for the calculation.AIPC periodica, Zurich, S-16/81, 1981.

[20] S. Somayaji, S. P. Shah, Bond stress versus slip relationship and cracking response of tension members. J. Am. Concr. Inst., pp. 217-225, May-June 1981.

[21] S. Morita, T. Kaku, Cracking and deformation of reinforced prisms subjected to tension. Colloquium IABSE-FIP-CEB-RILLEM-IASS, Behaviour of concrete structures, Liège, II-3-2, pp. 583-594, 1975.

[22] M. Saad, Influence du pourcentage d'acier sur le comportement Post - fissuration du béton armé en traction. PhD thesis, University of Mouloud Mammeri of Tizi-Ouzou, Algeria, 2011.

[23] M. Saad, Y. Bouafia, M. S. Kachi, Contribution à l'évaluation d'ouverture des fissures dans les éléments en béton armé. Annales du Bâtiment et des Travaux Publics, n°4, pp. 102-114, 2014, ISSN : 1270-9840, CPPAP : 1002T77866, Ed. ESKA.

[24] M. L. P. Brice, Idées générales sur la fissuration du béton armé et du béton précontraint. Annales de l'I.T.B.P.T.P., n° 198, juin 1964.

[25] J. Trinh, Comportement de panneau en béton armé sollicité en traction simple dans son plan. C.E.B.T.P, Service d'étude des structures, Rapport interne, Nov. 1986.

[26] T. P.Tassios, J. Yannopoulos, Etude analytique sur l'adhérence acier-béton et la fissuration du béton armé sous charges cycliques. Annales de l'I.T.B.P.T.P., n° 393, Avril 1981.

[27] M. Saad, M. S. Kachi., Y. Bouafia,P. Muller, B. Fouré, Influence du pourcentage d'acier sur le comportement du béton tendu fissuré- Calcul de l'ouverture des fissures par le biais de « l'acier fictif». E.J.E.C.E., European Journal of Environmental and Civil Engineering, Vol. 14, n° 3, pp. 303-327, 2010.

Annex 1:

Nomenclature

f_{ctm} : concrete average tensile strength
g : relative slip between steel and concrete (g = uc - us)
g_1 : value of the slip corresponding to the peak of the steel-concrete adhesion law (CEB)
τ: bond slip shear between steel and concrete
τ_1: maximum bond slip shear between steel and concrete
n : equivalence coefficient n = Es/Ec

p : total perimeter of steel reinforcement
$_c, u_s$: respectively elongation of concrete and steel
A_s, A_c: respectively, steel and concrete cross-sections
E_c, E_s: respectively concrete and steel elastic moduli
N_t: external applied tensile force,
N_r : tensile force in the cracked stage
α : exponent of the slip-adhesion law proposed by the model code CEB 1990
γ : total number of main cracks in the RC element
ρ : steel reinforcement ratio
σ_c: concrete normal stress
σ_{cr}: concrete effective tensile strength
σ_{ci}: concrete tensile strength at the ith crack
σ_e: steel yield strength
σ_s : steel tensile stress
$\sigma_{s\gamma}$: normal stress of the steel at the last crack γ
σ_{sf}: normal stress of the steel at the crack
σ_{sr}: normal stress of steel at the appearance of the first crack
$\Delta\varepsilon_m$(or $\Delta\varepsilon$) : tension stiffening effect of concrete lying between two successive cracks
L : total length of the considered RC element
L_0 : sum of the lengths (l_0) of the disturbed zones of the RC element
L_h : length or sum of the lengths of the homogenized zones of the RC element
L_t : sum of the total introduction lengths (l_t) of the RC element
l_0: disturbed length on either side of a crack($l_0 = \delta l_t$)
l_{a1} : effective introduction length at crack stabilization ($\lambda < 2l_t$) when g (l_0) <g_1
l_1: effective introduction length when the slip g at the distance l_0 remains lower than g_1 (with $\lambda > 2l_t$)
l_t : total introduction length
$l_{t1} := (l_0 + l_1)$, total introduction length when sliding at distance l_0 of the crack is lower than g1 (with$\lambda > 2l_t$)
l_{ta1} : total introduction length at crack stabilization ($\lambda < 2l_t$)) when g (l_0) <g_1
l_{1r} : length (noted with an index r) relative to the appearance of the first crack corresponding to the length l_1.
l_{t1r} : total introduction length (with an index r) relative to the appearance of the first crack corresponding to the length l_{t1}.
ε_e: steel elastic strain limit
ε_m: mean strain of the RC element
$\varepsilon_s, \varepsilon_c$: respectively, steel and concrete strains
ε_{sf}: steel strain in the cracked stage
ε_{sfa1} : steel strain in the cracked stage corresponding to the introduction length l_{ta1}.
$\varepsilon_{sm\lambda}$: mean steel strain at crack stabilization corresponding to average crack spacing λ
ε_{sm1}, ε_{cm1}: respectively mean steel and concrete strains corresponding along the introduction length l_1
ε_{sma1}, ε_{cma1} : respectively mean steel and concrete strains corresponding along the introduction length l_{a1}
ε_{smt1}, ε_{cmt1}: respectively mean steel and concrete strains corresponding along the introduction length l_{t1}
ε_{smta1}, ε_{cmta1}1: respectively mean steel and concrete strains corresponding along the introduction length l_{ta1}
$\varepsilon_{sr}, \varepsilon_{cr}$: respectively steel and concrete strains at the first crack
λ, λ_1: distance between two successive cracks corresponding, respectively, to the introduction lengths l_t and l_{t1}
$\bar{\lambda}$: ($= 1{,}7\ l_{tr}$) average spacing between two successive cracks at the crack stabilization state

$\bar{\lambda}_1 (= 1.7 l_{t1r})$ average spacing between two successive cracks at the crack stabilization state corresponding to the introduction length l_{t1r}